Supplementary materials

Zhanjie Gao, Sandeep Golla, Rajath Sawant, Vladimir Osipov, Gauthier Briere, Stephane Vezian, Benjamin Damilano, Patrice Genevet*, and Konstantin E. Dorfman*

Revealing topological phase in Pancharatnam-Berry metasurfaces using mesoscopic electrodynamics

S1 Electrodynamics of metasurface

S1.1 Lattice model for light-metasurface interaction

The classical formulation of the light scattering problem is based on the Maxwell's equations without external currents and charges [1]

$$\nabla \cdot \boldsymbol{D} = 0, \tag{S1}$$

$$\nabla \times \boldsymbol{E} = -\frac{1}{c}\frac{\partial \boldsymbol{B}}{\partial t}, \tag{S2}$$

$$\nabla \cdot \boldsymbol{B} = 0, \tag{S3}$$

$$\nabla \times \boldsymbol{H} = \frac{1}{c}\frac{\partial \boldsymbol{D}}{\partial t}. \tag{S4}$$

We restrict ourself by considering non-magnetic media, so that the magnetic and diamagnetic fields are equal (the vacuum electric and magnetic permittivity are set to unity), $\boldsymbol{B} = \boldsymbol{H}$. Following the standard Maxwell's equations notations, we use the vector of polarization, $\boldsymbol{D} = \boldsymbol{E} + 4\pi\boldsymbol{P}$. Therefore the system of Maxwell's equations are given by Eq. (1) in the main text. Information about the matter is solely contained in the functional dependence of $\boldsymbol{P}$ on $\boldsymbol{E}$. The geometry of the system is chosen such that z axis of the laboratory coordinate system can be directed along the normal to the surface and $\boldsymbol{\rho} = (x, y)$ is a two-dimensional vector in the plane of metasurface. Particular dependence of $\boldsymbol{P}$ on $\boldsymbol{E}$ is considered in the following sections. When the metasurface is placed at the interface between two isotropic media with different refractive incides, the corresponding z-dependent terms read

$$\boldsymbol{P}(z, \boldsymbol{\rho}, t) = \mathcal{H}(|z| \le l_z/2)\boldsymbol{P}(\boldsymbol{E}) + \mathcal{H}(z < -l_z/2)\chi_i \boldsymbol{E}(z, \boldsymbol{\rho}, t) + \mathcal{H}(z > l_z/2)\chi_t \boldsymbol{E}(z, \boldsymbol{\rho}, t). \tag{S5}$$

Here and below Heaviside function $\mathcal{H}(\text{condition}) = \{1, \text{ when condition is true; } 0, \text{ when condition is false}\}$. Then Eq. (1) in the main text for the domain $z < -l_z/2$ and $z > l_z/2$ describe the propagating waves with the effective speeds of light $c_i = c/n_i$ and $c_t = c/n_t$ where $n_{i,t} = \sqrt{1 + 4\pi\chi_{i,t}}$, respectively, denotes the refractive index of substrates on both side (see Fig. (S1)).

***Corresponding author: Konstantin E. Dorfman,** State Key Laboratory of Precision Spectroscopy, East China Normal University, Shanghai 200062, China, dorfmank@lps.ecnu.edu.cn and **Patrice Genevet,** Université Côte d'Azur, CNRS, CRHEA, rue Bernard Gregory, 06560 Valbonne, France, patrice.genevet@crhea.cnrs.fr

Zhanjie Gao, State Key Laboratory of Precision Spectroscopy, East China Normal University, Shanghai 200062, China

Vladimir Osipov, State Key Laboratory of Precision Spectroscopy, East China Normal University, Shanghai 200062, China; H.I.T.-Holon Institute of Technology, 52 Golomb Street, POB 305 Holon 5810201, Israel

Sandeep Golla, Rajath Sawant, Gauthier Briere, Stephane Vezian, Benjamin Damilano, Université Côte d'Azur, CNRS, CRHEA, rue Bernard Gregory, 06560 Valbonne, France

Zhanjie Gao, and **Sandeep Golla** contributed equally to this work.

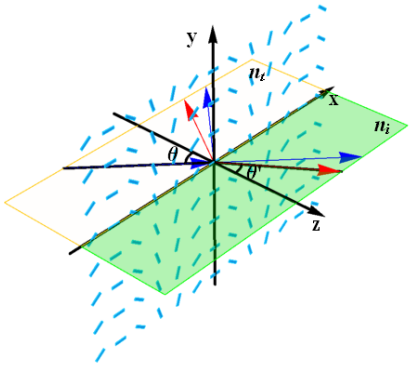

Fig. S1: Schematics of the reflection and refraction from the metasurface. The blue arrows represent the incidence light at the angle θ, ordinary refraction at the angle θ' and the ordinary reflection. The red arrows are the same but for the anomalous refraction and reflection.

The polarization in Eq. (1) vanishes in vacuum, and has non-zero values inside the media, which represents the thin layer of metasurface. We consider a classical linear response model for the metasurface $\boldsymbol{P}(z,\boldsymbol{\rho},t) = \chi(\boldsymbol{\rho})\boldsymbol{E}(z,\boldsymbol{\rho},t)$.

The Fourier transformation of the fields over $\boldsymbol{\rho}$ are defined as follows:

$$\boldsymbol{E}(z,\boldsymbol{\kappa},\omega) = \int d^2\boldsymbol{\rho}dt\boldsymbol{E}(z,\boldsymbol{\rho},t)e^{-\mathrm{i}\boldsymbol{\kappa}\cdot\boldsymbol{\rho}+\mathrm{i}\omega t}, \quad \boldsymbol{E}(\boldsymbol{r},t) = \frac{1}{(2\pi)^3}\int d^2\boldsymbol{\kappa}d\omega\boldsymbol{E}(z,\boldsymbol{\kappa},\omega)e^{\mathrm{i}\boldsymbol{\kappa}\cdot\boldsymbol{\rho}-\mathrm{i}\omega t}. \tag{S6}$$

Polarization is expressed in terms of the field,

$$\boldsymbol{P}(z,\boldsymbol{\kappa},\omega) = \frac{1}{(2\pi)^2}\int d^2\boldsymbol{\kappa}'\tilde{\chi}(\boldsymbol{\kappa}-\boldsymbol{\kappa}')\boldsymbol{E}(z,\boldsymbol{\kappa}',\omega), \quad \tilde{\chi}(\boldsymbol{\kappa}) = \int d^2\boldsymbol{\rho}\chi(\boldsymbol{\rho})e^{-\mathrm{i}\boldsymbol{\kappa}\boldsymbol{\rho}}. \tag{S7}$$

The linear susceptibility function $\chi(\boldsymbol{\rho})$ is a periodic function of coordinates. It can be represented as a sum of the susceptibilities of the individual primitives shifted and rotated in xy plane. The reflection and transition is therefore defined by the vectors of the reciprocal lattice $\boldsymbol{G}$, where the function $\chi(\Delta\boldsymbol{\kappa})$ reaches its maxima.

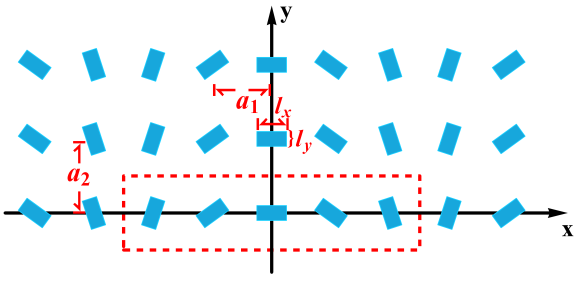

Fig. S2: Schematics of the metasurface. The length and width of the antenna are l_x and l_y, respectively. The distance between the two antennas in x and y axis are a_1 and a_2, respectively. Along the x axis, for $M = 5$ (shown here) the antennas are rotated by the angle $\phi = \frac{-\pi}{(2N+1)}$.

S1.2 Metasurface with translational symmetry

Since the length of the antenna is in the sub-wavelength scale and the metasurface is translation-invariant without considering the rotation of the antenna, as shown in Fig. S2, the susceptibility function $\chi(\boldsymbol{\rho})$ can be represented by

$$\chi(z,\boldsymbol{\rho}) = \chi_0 \sum_{mn} \sum_{j=-N}^{N} \Omega(\boldsymbol{\rho} - \boldsymbol{\varrho}_{Mm+j,n}), \quad \chi_0 = \begin{pmatrix} \chi_x & 0 \\ 0 & \chi_y \end{pmatrix}, \tag{S8}$$

where $N = (M-1)/2$ with the number of elements in the unit cell M, and the susceptibilities of the nanopillar along x and y directions are $\chi_x = [4\pi\omega - 4\pi\omega_0(1 - \frac{\sin^2(\theta)}{n_{eff}^2})^{-1/2}]^{-1}$, $\chi_y = [4\pi\omega - 4\pi\omega_1(1 - \frac{\cos^2(\theta)}{n_{eff}^2})^{-1/2}]^{-1}$ with different resonance frequencies ω_0 and ω_1 [2], effective refractive index of the nanopillar n_{eff} and incident angle θ. The indicator function $\Omega(\boldsymbol{\rho})$ describes the basic geometric primitive, which has a rectangular shape:

$$\Omega(\boldsymbol{\rho}) = \mathcal{H}(|x| \le l_x/2)\mathcal{H}(|y| \le l_y/2). \tag{S9}$$

The lattice translation vector is $\boldsymbol{\varrho}_{m,n} = m\boldsymbol{a}_x + n\boldsymbol{a}_y$ with lattice primitive translation vectors $\boldsymbol{a}_x = (2N+1)a_1\boldsymbol{e}_x$ and $\boldsymbol{a}_y = a_2\boldsymbol{e}_y$. 2D spatial Fourier transformation of Eq. (S8) is

$$\tilde{\chi}(\boldsymbol{\kappa}) = \chi_0 \sum_{n} e^{-\mathrm{i}n\boldsymbol{\kappa}\boldsymbol{a}_2} \sum_{m} \sum_{j=-N}^{N} \tilde{\Omega}_{mnj}(\boldsymbol{\kappa})\, e^{-\mathrm{i}((2N+1)m+j)\boldsymbol{\kappa}\boldsymbol{a}_1}, \tag{S10}$$

where $\tilde{\Omega}_{mnj}(\boldsymbol{\kappa})$ is the Fourier transform of $\Omega(\boldsymbol{\rho} - \boldsymbol{\varrho}_{Mm+j,n})$. Since the rotation of antenna in one unite cell is treated by the rotation of the transmission matrix later by the form $\hat{\tilde{T}}'(\phi_j) = \hat{R}^\dagger(\phi_j)\hat{\tilde{T}}\hat{R}(\phi_j)$ in the main text, all the $\tilde{\Omega}_{mnj}(\boldsymbol{\kappa})$ with different indexes m, n, j are same and the subscripts mnj will be omitted below. By using the Poisson summation formula $\sum_{n'=-\infty}^{\infty} F(k - 2\pi n'a) = \frac{1}{2\pi a} \sum_{n=-\infty}^{\infty} \hat{F}(\frac{n}{2\pi a}) e^{-\mathrm{i}kn/a}$ where $\hat{F}$ is the Fourier transformation of F, Eq. (S10) reduce to

$$\tilde{\chi}(\boldsymbol{\kappa}) = \sum_{m',n'} \delta\left(\kappa_x - \frac{2\pi m'}{(2N+1)a_1}\right) \delta\left(\kappa_y - \frac{2\pi n'}{a_2}\right) F_{m'n'}, \tag{S11}$$

where $F_{m'n'} = \frac{\chi_0(2\pi)^2}{(2N+1)a_1a_2} \sum_{j=-N}^{N} \tilde{\Omega}(\boldsymbol{\kappa})\, e^{-\mathrm{i}j\boldsymbol{\kappa}\boldsymbol{a}_1}$. Taking the inverse Fourier transform, we obtain

$$\tilde{\chi}(\boldsymbol{\rho}) = \frac{\chi_0}{(2N+1)a_1a_2} \sum_{m',n'} \sum_{j=-N}^{N} \tilde{\Omega}(\boldsymbol{G}_{m'n'}) e^{\mathrm{i}\boldsymbol{G}_{m'n'}\cdot(\boldsymbol{\rho} - j\boldsymbol{a}_1)},$$

where the reciprocal lattice vector $\boldsymbol{G}_{m'n'} = \frac{2\pi m'}{(2N+1)a_1}\boldsymbol{e}_x + \frac{2\pi n'}{a_2}\boldsymbol{e}_y$. Substitution of the result (S11) into (S7) produces the series for the polarization vector

$$\boldsymbol{P}(z,\boldsymbol{\kappa},\omega) = \frac{\chi_0}{(2N+1)a_1a_2} \sum_{m',n'} \sum_{j=-N}^{N} \int d^2\boldsymbol{\kappa}'\, \delta\left(\boldsymbol{\kappa} - \boldsymbol{\kappa}' - \boldsymbol{G}_{m',n'}\right) e^{-\mathrm{i}j(\boldsymbol{\kappa}-\boldsymbol{\kappa}')\boldsymbol{a}_1} \tilde{\Omega}(\boldsymbol{\kappa} - \boldsymbol{\kappa}')\boldsymbol{E}(z,\boldsymbol{\kappa}',\omega). \tag{S12}$$

By taking inverse Fourier transform of Eq. (S12), polarization vector is given by Eq. (2) in the main text as a sum over the Brillouin zones. To define the nonuniform part of the system of Maxwell's equations, we assume that the incident light has the form $\boldsymbol{E}(z,\boldsymbol{\rho},t) = \boldsymbol{E}_i\, e^{\mathrm{i}k_{zi}z + \mathrm{i}\boldsymbol{\kappa}_i\boldsymbol{\rho} - \mathrm{i}\omega_i t}$ where $k_{zi} = \sqrt{\frac{\omega_i^2 n_i^2}{c^2} - \kappa_i^2}$ with the conditions $\omega_i n_i > c\kappa_i$. Since there are no other temporal characteristics except the ω_i, all the time-derivatives can be replaced by the multiplication by $-\mathrm{i}\omega_i$. We seek for the solution of the Maxwell's equations (1) in the form of Eq. (4) in the main text.

S1.3 Thin metasurface limit

In zeroth approximation, we assume that the surface polarization is caused by the incident light only, so that $\boldsymbol{P}_{||} = \chi \boldsymbol{E}_{in} e^{\mathrm{i}k_{zi} + \mathrm{i}\boldsymbol{\kappa}_i \boldsymbol{\rho}}$ and

$$\frac{\partial^2}{\partial z^2}\boldsymbol{E}_{||} + \nabla^2_{\boldsymbol{\rho}}\boldsymbol{E}_{||} + \frac{\omega_i^2 n_{i,t}^2}{c^2}\boldsymbol{E}_{||} = -4\pi\nabla_{\boldsymbol{\rho}}(\nabla_{\boldsymbol{\rho}}\cdot\boldsymbol{P}_{||}) - 4\pi\nabla_{\boldsymbol{\rho}}\frac{\partial}{\partial z}P_z - 4\pi\frac{\omega_i^2}{c^2}\boldsymbol{P}_{||}. \tag{S13}$$

The following equations are written for the $e^{\mathrm{i}(\boldsymbol{G}_{mn}+\boldsymbol{\kappa})\boldsymbol{\rho}}$ components of above equations. All the $\boldsymbol{G}_{mn}+\boldsymbol{\kappa}$ spatial components of the $\tilde{E}, \tilde{P}$ have the same subscripts m and n which will be further omitted. And the corresponding thin polarization component $\mathcal{H}(|z| \le l_z/2)\boldsymbol{P}(\boldsymbol{E})$ is

$$\tilde{\mathcal{H}}(\mathrm{k}_z)\boldsymbol{P}_{||}(\mathrm{k}_z, \boldsymbol{\kappa}) = \frac{\sin(\xi l_z)}{4\pi\xi}\chi_0 f_{mn}\boldsymbol{E}_{||,i}\delta(\boldsymbol{\kappa}_i - \boldsymbol{\kappa}) \simeq \frac{l_z}{4\pi}\chi_0 f_{mn}\boldsymbol{E}_{||,i}\delta(\boldsymbol{\kappa}_i - \boldsymbol{\kappa}), \tag{S14}$$

where $f_{m,n} = \sum_{j=-N}^{N} f_{mn,j} e^{-\mathrm{i}j\boldsymbol{G}_{mn}\boldsymbol{a}_1}$, $2\xi = k_{zi} - \mathrm{k}_z$, $\boldsymbol{E}_{||,i}$ is the x, y amplitudes of incident light. When the incident angle or the thickness of the antenna l_z is small which corresponds to $\xi \approx 0$ or $l_z \approx 0$, then $\frac{\sin(\xi l_z)}{\xi} \approx l_z$. Considering the thickness of the metasurface to be small, we neglect the E_z and P_z components in the model and obtain

$$\frac{1}{2\pi}\left(\frac{\omega_i^2 n_{i,t}^2}{c^2} - K_{||}^2 - \mathrm{k}_z^2\right)\tilde{E}_x(\mathrm{k}_z, \boldsymbol{\kappa}) = \left(K_x^2 - \frac{\omega_i^2}{c^2}\right)\tilde{P}_x + K_x K_y \tilde{P}_y, \tag{S15}$$

$$\frac{1}{2\pi}\left(\frac{\omega_i^2 n_{i,t}^2}{c^2} - K_{||}^2 - \mathrm{k}_z^2\right)\tilde{E}_y(\mathrm{k}_z, \boldsymbol{\kappa}) = \left(K_y^2 - \frac{\omega_i^2}{c^2}\right)\tilde{P}_y + K_y K_x \tilde{P}_x, \tag{S16}$$

where $K_x = G_{mn,x} + \kappa_x$, $K_y = G_{mn,y} + \kappa_y$, $K_{||}^2 = (G_{mn,x} + \kappa_x)^2 + (G_{mn,y} + \kappa_y)^2$, $\tilde{E}_y(\mathrm{k}_z, \boldsymbol{\kappa}), \tilde{E}_y(\mathrm{k}_z, \boldsymbol{\kappa})$ are function of $\mathrm{k}_z, \boldsymbol{\kappa}$ need to be calculated, $\tilde{\boldsymbol{P}}_{||} = l_z\chi_0 f_{mn}\boldsymbol{E}_{||,i}\delta(\boldsymbol{\kappa}_i - \boldsymbol{\kappa})$.

S2 Reflection and refraction from metasurfaces with translational symmetry

S2.1 Transmission matrix

We can now investigate how the light is transmitted through the metasurface. In the present model, we assume that, for a typical design, individual primitives are spaced sparsely which eliminates a possibility of the inter-element interactions. In this case, one can calculate the transmission through the individual primitive and then sum over all the elements of the unit cell and the entire metasurface. Consider the rectangular primitive with perfectly aligned sides along x and y coordinates such that the long side l_y is along the y-axis and the short side l_x is along the x-axis. We can thus recast Eqs. (S15) - (S16) in terms of the transmission matrix $\hat{\tilde{T}}$ given by Eq. (4) in the main text (Due to $e^{-\mathrm{i}j\boldsymbol{G}_{mn}\boldsymbol{a}_1}$ is included in the propagation phase $\psi_{mn,j}$, we omitted it in here.):

$$\begin{pmatrix} \tilde{E}_{x,m,n} \\ \\ \tilde{E}_{y,m,n} \end{pmatrix} = \begin{pmatrix} \tilde{t}_{xx} & \tilde{t}_{xy} \\ \\ \tilde{t}_{yx} & \tilde{t}_{yy} \end{pmatrix} \begin{pmatrix} E_{xi} \\ \\ E_{yi} \end{pmatrix},$$

where the elements of transmission matrix are given by

$$\begin{aligned}
\tilde{t}_{xx} &= \frac{\tilde{C}'_r}{\tilde{C}'}(K_x^2 - \frac{\omega_i^2}{c^2})\chi_x, \\
\tilde{t}_{xy} &= \frac{\tilde{C}'_r}{\tilde{C}'}(K_x K_y)\chi_y, \\
\tilde{t}_{yx} &= \frac{\tilde{C}'_r}{\tilde{C}'}(K_x K_y)\chi_x, \\
\tilde{t}_{yy} &= \frac{\tilde{C}'_r}{\tilde{C}'}(K_y^2 - \frac{\omega_i^2}{c^2})\chi_y.
\end{aligned} \tag{S17}$$

Here $\tilde{C}' = -\mathrm{k}_z^2 + \frac{\omega_i^2 n_{i,t}^2}{c^2} - K_{||}^2$, $\tilde{C}'_r = 2\pi l_z f_{mn,j}\delta(\boldsymbol{\kappa}_i - \boldsymbol{\kappa})$, $\boldsymbol{\kappa}_i < \boldsymbol{G}_{1,1} = \frac{2\pi}{(2N+1)a_1}\boldsymbol{e}_x + \frac{2\pi}{a_2}\boldsymbol{e}_y$. In the physical space, the transmission matrix $\hat{T}$ can be written as

$$\begin{aligned}
t_{xx} &= \frac{C'_r}{C'}(K_x^2 - \frac{\omega_i^2}{c^2})\chi_x, \\
t_{xy} &= \frac{C'_r}{C'}(K_x K_y)\chi_y, \\
t_{yx} &= \frac{C'_r}{C'}(K_x K_y)\chi_x, \\
t_{yy} &= \frac{C'_r}{C'}(K_y^2 - \frac{\omega_i^2}{c^2})\chi_y,
\end{aligned} \tag{S18}$$

where $C' = \sqrt{\frac{\omega_i^2 n_{i,t}^2}{c^2} - K_{||}^2}\big|_{\boldsymbol{\kappa}=\boldsymbol{\kappa}_i}$, $C'_r = \mathrm{i}l_z f_{mn,j}/4\pi|_{\boldsymbol{\kappa}=\boldsymbol{\kappa}_i}$.

S3 Derivation of the Fresnel coefficient

So far we have investigated the transmission properties of the metasurfaces assuming that the incident and transmitted light are polarized linearly. We now consider a circularly polarized (CP) light. We therefore have to transform the solution to the CP basis $\sigma_\pm = (\boldsymbol{e}_x \cos(\theta') \pm \mathrm{i}\boldsymbol{e}_y)/\sqrt{2}$, where θ' is the refraction angle (see Fig. S1). For an ordinary operator $\hat{A}$ in the linear polarization basis, we define an operator $\hat{\tilde{A}}$ in the CP basis $\hat{A}\frac{(x,y)\to(\sigma_\pm)}{}\hat{\tilde{A}}$. For instance, the rotation operator $\hat{R}(\phi_j)$ defined in Eq. (6) can be recast in the circular polarization basis as an operator $\hat{\tilde{R}}(\phi_j)$ defined as follows

$$\hat{\tilde{R}}(\phi_j) = \begin{pmatrix} \frac{e^{\mathrm{i}\phi_j}(2-\sec\theta'-\cos\theta')+e^{-\mathrm{i}\phi_j}(2+\sec\theta'+\cos\theta')}{4} & \frac{e^{\mathrm{i}\phi_j}(\sec\theta'-\cos\theta')+e^{-\mathrm{i}\phi_j}(-\sec\theta'+\cos\theta')}{4} \\ \frac{e^{-\mathrm{i}\phi_j}(\sec\theta'-\cos\theta')+e^{\mathrm{i}\phi_j}(-\sec\theta'+\cos\theta')}{4} & \frac{e^{-\mathrm{i}\phi_j}(2-\sec\theta'-\cos\theta')+e^{\mathrm{i}\phi_j}(2+\sec\theta'+\cos\theta')}{4} \end{pmatrix}. \tag{S19}$$

Similarly the transmission matrix $\hat{T}$ in Eq. (5) takes the form

$$\hat{\tilde{T}} \equiv \begin{pmatrix} \frac{t_{yy}+t_{xx}-\mathrm{i}t_{xy}\cos\theta'+\mathrm{i}t_{yx}\sec\theta'}{2} & \frac{t_{yy}-t_{xx}-\mathrm{i}t_{xy}\cos\theta'-\mathrm{i}t_{yx}\sec\theta'}{2} \\ \frac{t_{yy}-t_{xx}+\mathrm{i}t_{xy}\cos\theta'+\mathrm{i}t_{yx}\sec\theta'}{2} & \frac{t_{yy}+t_{xx}+\mathrm{i}t_{xy}\cos\theta'-\mathrm{i}t_{yx}\sec\theta'}{2} \end{pmatrix}. \tag{S20}$$

We then consider the in plane transmission condition $t_{xy} = 0, t_{yx} = 0$. In the CP basis the corresponding operator reads

$$\hat{\tilde{T}}(\phi_j) = \begin{pmatrix} t'_{1j} & t'_{2j} \\ t'^*_{2j} & t'^*_{1j} \end{pmatrix}, \tag{S21}$$

where

$$t'_{1j} = \frac{4(t_{xx}+t_{yy}) + e^{\mathrm{i}2\phi_j}(t_{xx}-t_{yy})(\cos\theta' - \sec\theta') + e^{-\mathrm{i}2\phi_j}(t_{xx}-t_{yy})(\sec\theta' - \cos\theta')}{8},$$

$$t'_{2j} = \frac{e^{-\mathrm{i}2\phi_j}(t_{xx}-t_{yy})(2-\sec\theta'-\cos\theta') + e^{\mathrm{i}2\phi_j}(t_{xx}-t_{yy})(2+\sec\theta'+\cos\theta')}{8}.$$

The CP light with the incident angle θ can be recast as $\{\frac{1}{2}(\pm 1+\sec\theta'\cos\theta), \frac{1}{2}(\mp 1+\sec\theta'\cos\theta), 0\}$. The $E_{mn,j}$ component of the refracted light then reads

$$E_{mn,j} = \begin{pmatrix} E_{+1} + E_{+2}e^{-\mathrm{i}2\phi_j} + E_{+3}e^{\mathrm{i}2\phi_j} \\ \\ E_{-1} + E_{-2}e^{-\mathrm{i}2\phi_j} + E_{-3}e^{\mathrm{i}2\phi_j} \end{pmatrix} F_{mn,j}, \tag{S22}$$

where

$$\begin{aligned}
E_{+1} &= \frac{(t_{xx}+t_{yy})(\cos\theta\sec\theta' \pm 1)}{4}, E_{+2} = \frac{(t_{xx}-t_{yy})(\cos\theta\pm 1)(\sec\theta'-1)}{8}, \\
E_{+3} &= \frac{(t_{xx}-t_{yy})(\cos\theta\mp 1)(\sec\theta'+1)}{8}, \\
E_{-1} &= \frac{(t_{xx}+t_{yy})(\cos\theta\sec\theta' \mp 1)}{4}, E_{-2} = \frac{(t_{xx}-t_{yy})(\cos\theta\pm 1)(\sec\theta'+1)}{8}, \\
E_{-3} &= \frac{(t_{xx}-t_{yy})(\cos\theta\mp 1)(\sec\theta'-1)}{8}.
\end{aligned} \tag{S23}$$

Consider the general refraction law, the refraction angle satisfies $\sin\theta' = \frac{m\lambda}{5a_1 n_{i,t}} + \frac{n_i\sin\theta}{n_{i,t}}$ where $m = 0, \pm 1$. Using the field amplitudes in the circular polarization basis $E^{\pm s} = (\boldsymbol{e}_x\cos(\theta') \pm s\mathrm{i}\boldsymbol{e}_y)/\sqrt{2}$, which yields the general result:

$$E = \sum_{mnj}(E_1 + E_2 e^{-s\mathrm{i}2\phi_j} + E_3 e^{s\mathrm{i}2\phi_j})F_{mn,j} \tag{S24}$$

with E_1, E_2, E_3 can be written as Eq. (9) where

$$\begin{aligned}
t_{1\pm} &= \frac{(t_{xx}+t_{yy})(\cos\theta\sec\theta'\pm 1)}{4}, \\
t_{2\pm\pm} &= \frac{(t_{xx}-t_{yy})(\cos\theta\pm 1)(\sec\theta'\pm 1)}{8}, \\
E^{\pm s} &= (\boldsymbol{e}_x\cos(\theta') \pm s\mathrm{i}\boldsymbol{e}_y)/\sqrt{2}.
\end{aligned} \tag{S25}$$

Since $l_y << \lambda$ and $l_x < \lambda$, then $t_{yy} \propto \chi_y$ can be neglected. In order to get a more clear and simper analytic expression without effect physical picture, we discuss a 1D model in the following. Consider $t_{xx} = \frac{\mathrm{i}f_{mn,j}l_z\chi_x(K_x^2 - \frac{\omega_i^2}{c^2})}{2\sqrt{\frac{\omega_i^2 n_{i,t}^2}{c^2} - K_x^2}} \approx t'_{xx}\cos\theta'$ where $t'_{xx} = \frac{-\mathrm{i}f_{mn,j}l_z\chi_x}{2}$ and the refractive indexes in two sides of the metafursace are close $n_i = n_t \approx 1$, then E_1, E_2, E_3 can be written as

$$\begin{aligned}
E_1 &= t'_{1+}E^s + t'_{1-}E^{-s}, \\
E_2 &= t'_{2-+}E^s + t'_{2++}E^{-s}, \\
E_3 &= -t'_{2+-}E^s - t'_{2--}E^{-s},
\end{aligned} \tag{S26}$$

where

$$\begin{aligned}
t'_{1\pm} &= \frac{1}{4}t'_{xx}(\cos\theta \pm \cos\theta'), \\
t'_{2\pm\pm} &= \frac{1}{8}t'_{xx}(\cos\theta\pm 1)(\cos\theta'\pm 1).
\end{aligned} \tag{S27}$$

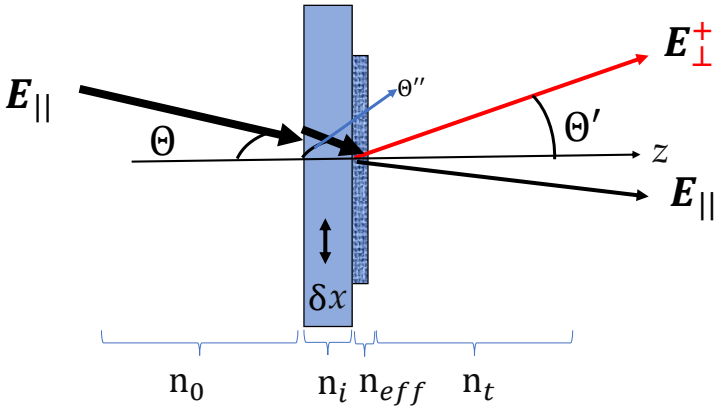

Fig. S3: Schematic of the light transmission through the PB metasurface.

It is clear that the amplitude of different components satisfy $|t'_{1+}| >> |t'_{2-+}|, |t'_{2+-}|$ and $|t'_{2++}| >> |t'_{1-}|, |t'_{2--}|$, when the incident and refracted angles are small. The transmission light is therefore given by

$$E = \sum_{mnj} (t'_{1+} E^s + t'_{2++} E^{-s} e^{-\mathrm{si}2\phi_j}) F_{mn,j}.$$

Combining with the constant phase term $e^{2\mathrm{i}m\phi_j}$ in $F_{mn,j}(z,\rho)$ (antennas are rotated in a clockwise direction in Fig. S2), for RCP incident light ($s = 1$), only $m = 0, 1$ order components can be refracted; for LCP incident light ($s = -1$), only $m = 0, -1$ order components can be transferred due to the averaging out of the phase components $\sum_j e^{\pm \mathrm{i}2\phi_j} \simeq \sum_j e^{\pm \mathrm{i}4\phi_j} \simeq 0$.

S3.1 Derivation of the transmission efficiency

In order to describe experimental observations, the details of theoretical model are presented as follows. As shown in the Fig. S3, the transmission of the light traverses three medium: the air, the substrate, and the metasurface.

We first consider light transmission through the air/substrate interface. Refraction angle satisfies ordinary Snell's law: $\frac{\sin(\theta'')}{\sin(\theta)} = \frac{n_0}{n_i}$ where n_0 and n_i are the refractive indexes of air and substrate, respectively. The x and y components of the electric field in the substrate satisfy the Fresnel formula

$$E_x = \frac{2\cos(\theta)^2}{\sqrt{2}[\cos(\theta) + n_2\cos(\theta'')]}, \quad E_y = \frac{i2\cos(\theta)}{\sqrt{2}[\cos(\theta'') + n_2\cos(\theta)]}.$$

After passing through the substrate light interacts with the metasurface where the refraction is described by the generalized Snell's law and the amplitude obeys Eq. (10) of the main text. In order to model the structural birefringence of the rectangular nano pillars, the x nd y components of the susceptibility tensor of GaN nanopillar are defined after Eq. (S8), which agrees with angle resolved photoluminescence experiments of the birefringent material. In addition, by expanding the angle-dependent susceptibility components in a Taylor series, one can obtain an angular dispersion similar to that observed in THz metasurfaces [3], where the phenomenological amplitudes in the expansion represent inter-particle coupling strengths. The transmission through the metasurface is further described by our mesoscopic model (see Eq. (10)), which allows us to obtain the final anomalous refraction efficiency.

S4 Design of the polarization dependent beam splitter

The interferometric measurement between normal and anomalous refraction imposes that the scattering properties of the interface should contain both zero and first diffraction order with similar amplitude and polarization. The latter can be addressed by inserting a quarter wave plate into the path of the one of the diffracted beams. The former condition requires tuning the antenna scattering parameter. The amplitude and phase responses of the nanopillars forming the PB metasurface are related to the length and width of the nanopillar with a constant height of 800 nm. To maximize the PB metasurface efficiency, the antenna should maximally convert the polarization from the opposite orthogonal circular polarization, thus introducing a phase shift between ordinary and extraordinary axis of a nanopillar [4]. However, in contrast to the previous PB metasurface works seeking for the high performance devices [5], we are herein interested in quantifying the PB phase from the self-referenced interferometric measurements. Proper design is achieved by considering birefrigent nanopillar introducing $\pi/2$ or $3\pi/2$ phase retardation, as indicated in Fig. 2A. To account for both tapering and to compensate for anisotropic etching, we choose the nanopillar size corresponding to $3\pi/4$ phase shift. To quantify the phase-shift of the light transmitted through the GaN nanopillars, we perform the electromagnetic simulations of the light transmission through a subwavelength array of nanopillars arranged in a square lattice. The metasurface consists of GaN nanopillar array on Sapphire (Al_2O_3) substrate. The refractive index for GaN has the following Sellmeier like relation [6]:

$$n_0(\lambda) = \sqrt{1 + \frac{A_0\lambda^2}{\lambda^2 - (\lambda_0^G)^2} + \frac{B_0\lambda^2}{\lambda^2 - (\lambda_0^H)^2}},$$

$$n_e(\lambda) = \sqrt{1 + \frac{A_e\lambda^2}{\lambda^2 - (\lambda_e^G)^2} + \frac{B_e\lambda^2}{\lambda^2 - (\lambda_e^H)^2}}.$$

Here, $A_0 = 0.213$, $B_0 = 3.988$, $A_e = 0.118$, $B_e = 4.201$, $\lambda_0^G = \lambda_e^G = 350nm$, $\lambda_0^H = 153nm$, $\lambda_e^H = 173.5nm$. For Sapphire (Al_2O_3), refractive index relation is referred from [7]. For $\lambda = 632.8$ nm, the design wavelength, $n = 1.766$. GaN has very small birefringence, which we decided to neglect as a first approximation. To avoid diffraction both in free space and in the substrate, we arranged the spacing between the elements with a subwavelength period of 320 nm. The simulations are performed using the FDTD using plane wave sources at $632.8nm$ wavelength polarized along x and y axis, impinging at normal incidence satisfying the perfectly matched layer (PML) conditions in the direction of the light propagation subject to periodic boundary conditions along all the in-plane directions. The use of PML boundary conditions in the propagation direction results in an open space simulation while in-plane periodic boundary conditions mimic a subwavelength array of the identical nanostructures.

In figure S4, the polarization-conversion efficiency of a single GaN nanopillar is obtained by FDTD simulation. A meta-atom is impinged with two plane waves sources (x and y-polarized) of varying wavelength from 480 nm to 680 nm with the interval of 20 nm. The other simulation conditions are kept same as in the design simulation. To perform interference measurements as described in the main text, the design of the element is chosen to diffract 50% of the incident light on cross polarization.

S5 Interpretation of the interferometric experiments

Note, that Eq. (12) shows that MZI detects the displacement phase. Technically the displacement phase is a propagation phase, also known as detour phase, since the measurement involves translational motion alone. However as has been already pointed out in the discussion following Eq. (7), the propagation phase contains two parts, one of which cancels out the PB phase yielding non vanishing first diffraction order. The detour phase is therefore a remaining part of the propagation phase which enters the Snell's law. Note, however, that due to the translational invariance and uniform distribution of PB phases in the unit cell,

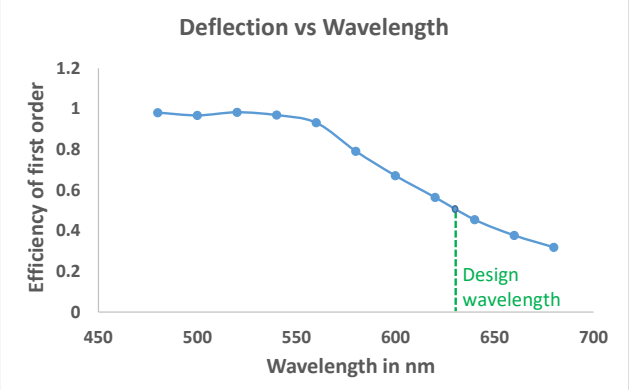

Fig. S4: Polarization conversion efficiency of a single GaN nanopillar.

the magnitude of the displacement phase is equivalent to the PB phase. This equivalence is not accidental and follows directly from the metasurface design itself, and therefore can be controlled at will. The MZI measurements thus provides although indirect yet unambiguous and conclusive measurement of the PB phase.

References

[1] Landau LD, Lifshitz EM. *Electrodynamics of continuous media*. (Pergamon, Amsterdam), Second edition, (1984).
[2] Houdre R, et al. Measurement of cavity-polariton dispersion curve from angle resolved photoluminescence experiments. *Phys Rev Lett* (1994);**73**:2043-2046.
[3] Qiu et al., Angular Dispersions in Terahertz Metasurfaces: Physics and Applications. *Phys Rev Appl* (2018);**9**:054050
[4] M Barbieri, G Vallone, P Mataloni, F De Martini. Complete and deterministic discrimination of polarization bell states assisted by momentum entanglement. *Phys Rev A* (2007);**75**:042317.
[5] Liu C, et al., Fully controllable pancharatnam-berry metasurface array with high conversion efficiency and broad bandwidth. *Sci Rep* (2016);**6**:34819-34819.
[6] S Pezzagna, J Brault, M Leroux, et al. Refractive indices and elasto-optic coefficients of GaN studied by optical waveguiding. *J Appl Phys* (2008);**103**:123112-123112.
[7] Palik ED, *Handbook of optical constants of solids* (Academic press, New York) (1984).

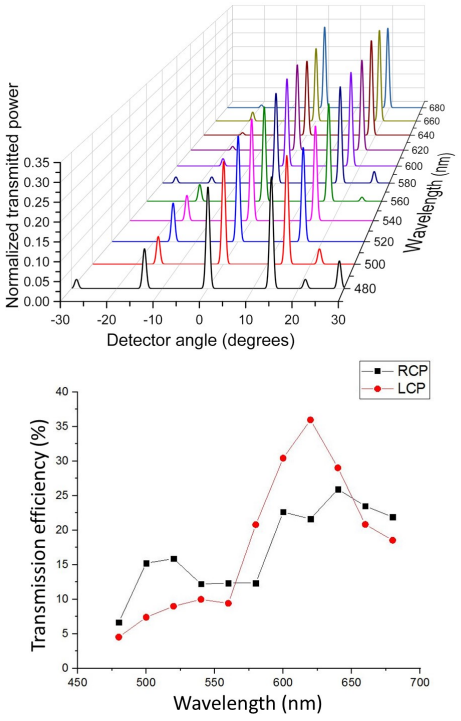

Fig. S5: Top: Measured angular deflection efficiency as a function of the incident wavelength for σ_+ incident polarization, to be compared with Fig 2D. Bottom: deflection efficiency as a function of the wavelength.